ChemComm

Thermo-Photo Hybrid Process for Steam Reforming of Methane: Highly Efficient Visible Light Photocatalysis

Journal:	*ChemComm*
Manuscript ID	CC-COM-05-2019-004193.R1
Article Type:	Communication

COMMUNICATION

Thermo-Photo Hybrid Process for Steam Reforming of Methane: Highly Efficient Visible Light Photocatalysis

Bing Han,[a] Wei Wei,[a] Meijia Li,[a] Kai Sun,[b] and Yun Hang Hu*[a]

Received 00th January 20xx,
Accepted 00th January 20xx

DOI: 10.1039/x0xx00000x

Steam reforming of methane (SRM) is one of the most important industrial processes, which produces 95% hydrogen used in USA. However, SRM is an endothermic reaction, which requires high energy input and high reaction temperature (>800 °C) for the current process. Furthermore, its products must be subjected to a water-gas shift (WGS) process. A photocatalytic process is expected to solve the energy issue and to eliminate the necessity of WGS for SRM. However, hydrogen yield from current photocatalytic steam reforming of methane (PSRM) is very small (μmol/h/g level), which is far below industrial interest. This work demonstrates that Pt/blackTiO$_2$ catalyst dispersed on light-diffuse-reflection-surface is excellent for efficient visible-light PSRM. Under visible light illumination on the catalyst by filtering UV light from AM 1.5G sunlight, the CH_4 and H_2O directly converted into H_2 and CO_2 without WGS, leading to a high H_2 yield of 185 mmol/h/g with a quantum efficiency of 60% at 500 °C. The yield is 3 orders of magnitude larger than the reported values, which can be attributed to the synergetic effect of potential and kinetic energies. This opens a new door for hydrogen production from water and natural gas with solar energy.

Hydrogen, which possesses the highest specific energy density, would be a promising fuel for future transportation, even though developing highly efficient techniques for on-board hydrogen storage and inexpensive fuel cells are still a challenge for the commercialization of fuel cell vehicles. Hydrogen is also an important feedstock for numerous industrial processes.[1] Currently, 95% of hydrogen used in United States is produced by steam reforming of methane (SRM):[2-5]

$$H_2O + CH_4 \rightarrow 3H_2 + CO \qquad \Delta H^o_{298}=206kJ/mol \qquad (Eq. 1)$$

Since methane is the most stable hydrocarbon, the endothermic SRM requires a high temperature to reach desired conversion rates of reactants with a large energy input.[3-5] Furthermore, in commercial hydrogen production,[5] CO/H_2 mixture product from SRM is subjected to a subsequent process called water gas shift (WGS, Equation 2) to enhance hydrogen yield.

$$CO+H_2O \rightarrow CO_2+H_2 \qquad \Delta H^o_{298}=-41kJ/mol \qquad (Eq. 2)$$

However, this increases the complexity of hydrogen production. Therefore, it is desirable to convert CH_4 and H_2O directly to H_2 and CO_2 as follows:

$$2H_2O + CH_4 \rightarrow 4H_2 + CO_2 \qquad \Delta H^o_{298}=165kJ/mol \qquad (Eq. 3)$$

However, this one-step process (eq. 3) is unlikely to be obtained with conventional thermocatalytic steam reforming of methane. This happens because the selectivity to produce $4H_2+CO_2$ (eq. 3) instead of $3H_2+CO$ (eq.1) thermodynamically prefers a low reaction temperature (Table S1 in Supplementary Information). In contrast, a high temperature is kinetically required to activate very stable CH_4 for a desired conversion rate. To solve the conflict requirement for operating temperature and the issue of high energy cost in thermocatalytic process, a photocatalytic approach with solar energy is very necessary.

Fujishima and Honda created a new era in heterogeneous photocatalysis by discovering the photoelectrocatalytic splitting of water in 1972.[6] As the most important photocatalyst, TiO_2 has been widely investigated. However, it can absorb only ultraviolet (UV) light (about 4% of the total solar energy) due to its relative large band gap energy (3.0~3.2 eV), leading to a low photo-conversion efficiency.[7-10] In the past 25 years, numerous pioneering contributions were made to extend the working spectrum of TiO_2 to visible-light region (which constitutes about 45% of the total solar energy).[7,11-17] As a breakthrough, Mao and his coworkers demonstrated that black TiO_2 synthesized by hydrogenating TiO_2 can remarkably absorb visible light.[7] However, the absorbed visible light by the black TiO_2 nanoparticles could not contribute to the photocatalytic process.[7,10] Very recently, we found that the inefficiency of

---

[a] Department of Materials Science and Engineering, Michigan Technological University, 1400 Townsend Drive, Houghton, MI 49931-1295, USA. *E-mail: yunhangh@mtu.edu.
[b] Department of Materials Science and Engineering, University of Michigan, Ann Arbor, MI, 48109-2136, USA.

Electronic Supplementary Information (ESI) available. See DOI: 10.1039/x0xx00000x

absorbed visible light for the photocatalytic H_2 production from water over black TiO_2 at room temperature was due to the kinetic limitation.[18] Furthermore, we demonstrated that this kinetic issue can be solved using an elevated temperature,[18] leading to a high visible light conversion efficiency for the CO_2 reduction with methane and the hydrogen production from water splitting.[18,19] So far, however, research on photocatalytic conversion of methane with water to chemicals and hydrogen fuel is in its infancy. For the direct synthesis of methanol from methane and liquid water under light illumination, several metal oxides, such as TiO_2 and WO_3, were explored as photocatalysts.[20,21] For hydrogen production from photocatalytic steam reforming of methane (PSRM), large-band-gap semiconductors (TiO_2, $NaTaO_3$/La, $CaTiO_3$, Ga_2O_3, or $K_2Ti_6O_{13}$) with a noble metal (Pt or Rh) have been employed as photocatalysts, which exploited only UV light (about 4% of the total solar energy), leading to a very low H_2 yield (at the level of μmol/h/g).[22,23] It is a long-time goal for photocatalytic processes to efficiently utilize visible light, since it accounts for ~45% of solar energy. In this work, we demonstrated that our invented catalyst system of Pt/blackTiO_2 catalyst on a light-diffuse-reflection surface is highly efficient for visible light photocatalytic steam reforming of methane (PSRM). Furthermore, the novel PSRM process can provide a very high hydrogen yield (199 mmol/h/g for 1.5 G sunlight and 185 mmol/h/g for visible light) at 500 °C, which is 1000 times larger than reported values at room temperature.

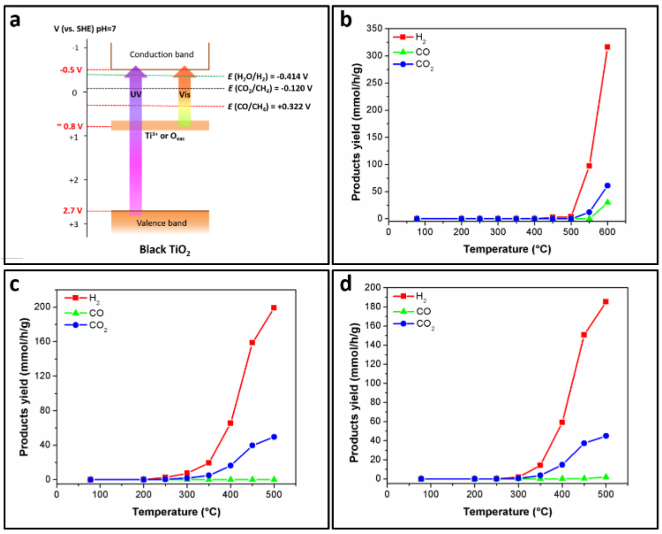

Fig. 1 Part I. Relationship between band structure of black TiO_2 and redox potentials of methane steam reforming: **(a)** The absorption of UV generates the excitation of electron from valance band of TiO_2 to its conduction band, whereas the absorption of visible light is associated with excitation of electrons from Ti^{3+} donor level to TiO_2 conduction band. **Part II.** Product yields from steam reforming of methane (H_2O/CH_4 molar ratio 1:1 and GHSV=80000 ml/h/g) over Pt/BlackTiO_2 catalyst dispersed on the light-diffuse-reflection-surface of a SiO_2 substrate: **(b)** without light irradiation; **(c)** under 1.5G sun light irradiation; and (**d**) under λ > 420 nm visible light irradiation.

It is well-known that an efficient visible light photocatalyst must meet three requirements: ability to absorb visible light, suitable band structure of a catalyst to match the redox potentials of a reaction, and high efficiency for light absorption. To meet those requirements, the Pt/blackTiO_2 catalyst on a light-diffuse-reflection-surface is considered as a promising catalyst system for the PSRM. First, this catalyst system can highly efficiently absorb light, since light absorption could be increased 100 times by dispersing photocatalyst particles on the light-diffuse surface of a SiO_2 substrate.[18] Second, different from pristine TiO_2 with a wide bandgap of about 3.2 eV (absorbing only UV light), black TiO_2 possesses a narrow bandgap of about 1.0 eV, which is small enough to absorb visible light and even near-IR.[7] Furthermore, we recently found that the absorbed visible light by black TiO_2 can contribute to photocatalysis at temperature above 200 °C.[18,19] Therefore, the Pt/blackTiO_2 catalyst is efficient for visible light absorption. Third, the band structure of black TiO_2 was evaluated (see band potential measurements in Supplementary information) and shown in Fig. 1a. One can see (a) H_2O/H_2 reduction potential is more positive than TiO_2 conduction band (CB) edge and (b) the oxidation potential of CO_2/CH_4 and CO/CH_4 is more negative than the energy level of the Ti^{3+}, which accounts for visible light absorption. This indicates that those energies meet the thermodynamic requirement for visible light PSRM over black TiO_2. To confirm the feasibility of this catalyst system for PSRM, the Pt/blackTiO_2 catalyst (15 mg) was prepared and dispersed on the light-diffuse-reflection-surface of a 4 cm^2 SiO_2 substrate. The obtained catalyst/substrate was loaded into a quartz tube reactor located in an electrical furnace (Fig. S3 in *Supplementary information*). The water/CH_4 mixture gas (GHSV=80000 ml/h/g) flow was introduced into the reactor and heated to a selected temperature. All products were analyzed by Gas Chromatograph (GC) and Mass Spectrometer (MS). The yields of products over the Pt/blackTiO_2 catalyst without light illumination was shown in Fig. 1b. The reaction hardly took place at 500 °C or below. When reaction temperature increased to 550 °C, the yield (97 mmol/h/g) of H_2 (with CO and CO_2 formation) was obtained. This is a typical thermocatalytic SRM, which needs a high operating temperature. To avoid thermocatalytic process, we select temperatures ≤ 500 °C for photocatalytic SRM. When the Pt/blackTiO_2 was irradiated by simulated AM 1.5 G sunlight, the reaction started at 200 °C, which is 300 °C lower than that without light illumination. H_2 yield increased with increasing temperature, leading to a high H_2 yield of 199 mmol/h/g at 500 °C. This impressive yield is about three orders of magnitude larger than reported results at room temperature[23]. Furthermore, the product of CH_4 oxidation is almost all CO_2 with negligible CO, leading to the molar ratio of 4 for H_2/CO_2 (Figs. 1c and 1d), which indicates the direct conversion of CH_4 and $2H_2O$ to $4H_2$ and CO_2 (Eq. 3). This can be explained as follows: In the photocatalytic SRM, the potential driving force to overcome the barrier of methane oxidation is the difference between the oxidation potential level of a methane and the potential level of Ti^{3+}. As shown in Figure 1a, one can see that the driving forces are about 0.478 and 0.920 eV for CH_4 oxidation to CO and CO_2, respectively. This suggests that the high selectivity for CO_2 formation with negligible CO is due to a larger driving force for CH_4 oxidation to CO_2 than to CO. Therefore, an additional reactor for WGS may not be needed for the photocatalytic SRM process. In addition, as shown in Fig. 2a, one can see that the apparent quantum efficiency (QE) for the entire AM 1.5G sunlight increased with increasing temperature, achieving the maximum value 65% at 500 °C.

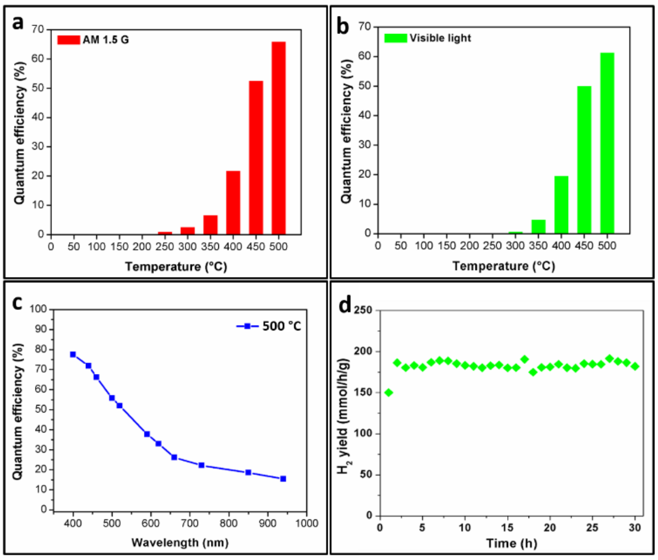

Fig. 2 Photocatalytic steam reforming of methane (H_2O/CH_4 molar ratio 1:1 and GHSV=80000 ml/h/g) over Pt/BalckTiO$_2$ catalyst dispersed on the light-diffuse-reflection-surface of a SiO_2 substrate: **(a)** Quantum efficiency vs reaction temperature under AM 1.5 G illumination, **(b)** Quantum efficiency vs reaction temperature under $\lambda > 420$ nm visible light illumination, **(c)** Quantum efficiencies vs wavelengths at 500 °C, and **(d)** H_2 yield vs reaction time under visible light ($\lambda > 420$ nm) illumination at 500 °C.

It is important to ensure that the light-enhanced H_2 yield over Pt/blackTiO$_2$ is only due to a photocatalytic process instead of the light-caused temperature increase. A high performance thermal imager was employed to acquire thermal images for the Pt/black TiO$_2$ dispersed on SiO_2 substrate. As shown in Fig. S4 (*Supplementary information*), one can see that the temperature of the catalyst bed without light illumination is uniform with 0.7~5.9 °C difference between maximum and minimum temperatures at various furnace-setting-temperatures. Under AM 1.5 G light illumination, the average temperature of the catalyst increased by only 4.7~8.1 °C. Furthermore, the catalyst temperature with light irradiation is also uniform just with 0.6~3.7 °C difference between maximum and minimum temperatures. This clearly demonstrated that the AM 1.5G light illumination did not create hot spots on the catalyst. Furthermore, although the increase in catalyst temperature caused by AM 1.5 G illumination was small (8.1 °C or less), the increased temperature was eliminated by reducing the electrical furnace heating. There was no difference of H_2 yield with and without light illumination over Pt/Al_2O_3 that is not a photocatalyst due to the large band gap energy of Al_2O_3 (>8eV) (Fig. S5 in *Supplementary information*). This clearly confirms that the light-enhanced H_2 yield over Pt/blackTiO$_2$ originates only from a photocatalytic process.

To evaluate the efficiency of visible light for the PSRM over Pt/blackTiO$_2$ catalyst dispersed on the light-diffuse-reflection-surface of a SiO_2 substrate, UV light ($\lambda < 420$ nm) was completely filtered from simulated AM 1.5G sunlight. Under visible light illumination, H_2 and CO_2 could be detected at temperature as low as 250 °C (Fig. 1d). Furthermore, H_2 yield increased with increasing temperature, reaching 185 mmol/h/g at 500 °C. Impressive apparent QE (49 % at 450 °C and 60% at 500 °C) were obtained for the entire visible light range (Fig. 2b). The photocatalytic activity under visible light was further confirmed by the relationship between QE and wavelength (Fig. 2c). Namely, the QE decreased monotonously with increasing wavelength for entire visible light range (from 400 to 940 nm). The catalyst stability for the visible light PSRM was also evaluated. As shown in Fig. 2d, one can see that hydrogen yield remained almost unchanged at 500 °C for 30 hours, indicating the excellent stability of the catalyst (Fig. 2d).

As discussed above, the remarkable effect of temperature on QE was observed for photocatalytic SRM, namely, QE increases with increasing reaction temperature (Figures 2a and 2b). It is well-known that increasing temperature can shorter the lifetime of excited electrons due to a faster recombination between excited electrons and holes, which decreases QE. However, the increased temperature enhances kinetic energy of reactants, which can accelerate their oxidation to donate electrons to the holes of the photocatalyst and their reduction to accept excited electrons from the photocatalyst, leading to the increase in QE.[18] In other words, the enhanced QE by increasing temperature indicates that the temperature effect is greater on redox reactions of reactants than on the electron-hole recombination in the photocatalytic SRM. This would be considered as synergetic effect between potential energy and kinetic energy. The activation of a reactant must overcome an energy barrier. In the photocatalytic SRM, the potential driving force to overcome the barrier for activation of methane and water can be attributed to the differences between the redox potential levels of reactants (methane and water) and the potential levels of the photocatalyst. However, kinetic energy (associated with temperature) is also a driving force to activate reactants, which was widely demonstrated in thermocatalytic processes. Because most of photocatalytic processes were carried out at ambient temperature, the effect of kinetic energy on photocatalytic process may be ignored. When the photocatalytic SRM was performed at an elevated temperature, the kinetic energy became large enough to play a role in the activation of methane and water. Therefore, at an elevated temperature, there is a synergetic contribution of potential energy and kinetic energy to the photocatalytic SRM, leading to an excellent photocatalytic performance.

The structures of Pt/BlackTiO$_2$ catalyst before and after photocatalytic SRM were characterized by various techniques. The electron paramagnetic resonance (EPR) measurements show a peak with g value of 1.97~1.98 (Fig. S8a), which is attributed to Ti^{3+} species.[24] Furthermore, the EPR peak intensity increased after photocatalytic SRM, indicating that the Ti^{3+} specials were not oxidized, which could make a contribution to the excellent stability of the catalyst (Fig. S8d). XPS, which is a surface characterization technique, shows only Ti^{4+} peaks (without Ti^{3+}) regardless of the reaction (Fig. S8b), indicating that there is not Ti^{3+} species in the surface layer. Therefore, the Ti^{3+} species are located inside the catalyst, which would be protected by the Ti^{4+} surface layer. This could explain why Ti^{3+} is stable in the photocatalytic SRM even at 500 °C. The visible light absorption by Ti^{3+} species generated photo-electrons, which can diffuse from the inside to the surface of the catalyst to reduce reactants. The high stability of the catalyst was further supported by XRD, which shows an unchanged diffraction pattern for the catalyst after the reaction (Fig. S8c). High resolution TEM was employed to evaluate microstructure of the catalyst. As shown in Figs. 3d and 3e, one can see that the TiO_2 particle sizes, which were originally ranged from 25 to 50 nm, slightly increased after the reaction. The average crystal particle size of TiO_2 (calculated from XRD patterns), which are almost same (28.6 and 27.5 nm, respectively) before and after the reaction, demonstrated the stable crystal structure of TiO_2. The apparent particles (with sizes of about 25-50 nm) observed from TEM images would be comprised of 1-2 primary crystal particles (about 28 nm). The Pt particle sizes are about 2-5 nm regardless of the reaction, indicating its excellent stability. Furthermore, the high resolution TEM image revealed that the exposed surface of the single crystal Pt particle is the cubic (111) plane (Fig. S8f). Those EPR, XPS, XRD, and TEM evaluations strongly support the excellent photocatalytic performance for SRM.

Temperature-dependence of TiO_2 band gap was evaluated using a high temperature UV-Visible spectrometer. It was found that the band gap between valence band (VB) and conduction band (CB) slightly and linearly decreased with increasing temperature (Fig.S7 in Supplementary information). Namely, when temperature was changed by 345 °C (from 25 to 370 °C), only 0.109 eV decrease in VB-CB energy gap (from 3.046 to 2.937 eV) was observed. Based on the obtained linear relationship between the band gap and temperature, the band gap of 2.908 eV was obtained at 500 °C. This indicates that only 0.138 eV in the band gap was decreased by increasing temperature from 25 to 500 °C. This small decrease in the VB-CB gap of TiO_2 was further supported by high temperature XRD measurements, in which the XRD pattern of TiO_2 remained unchanged with increasing temperature from room temperature to 500 °C. This indicates that interatomic spaces in TiO_2 remained almost unchanged with increasing temperature. It is well-known that the VB-CB bandgap of semiconductors tends to decrease with increasing temperature due to interatomic spacing increases. Therefore, with increasing temperature from 25 to 500 °C, the unchanged interatomic spaces support a very little change of the band gap for TiO_2.

A highly efficient visible-light photocatalytic steam reforming of methane (PSRM) was demonstrated with Pt/blackTiO_2 catalyst dispersed on light-diffuse-reflection-surface. Under visible light illumination by filtering UV light from AM 1.5G sunlight, H_2 yield can reach 185 mmol/h/g, with a quantum efficiency of 60% at 500 °C (Fig.2). The impressive yield is 3 orders of magnitude larger than reported values. Furthermore, the unique catalyst system can allow PSRM to achieve the direct conversion of CH_4 and $2H_2O$ to $4H_2$ and CO_2 without additional water-gas shift reaction. This brings a bright future for hydrogen production from water and natural gas with solar energy.

This work was partially supported by U.S. National Science Foundation (CBET-0931587 and CMMI-1661699). Authors also thanks Charles and Carroll McArthur for their great support.

Conflicts of interest

There are no conflicts to declare.

AUTHOR CONTRIBUTION

Y.H.H. designed the process. B.H. synthesized catalysts and materials, tested their photocatalytic performance, and carried out some characterization. W.W. conducted the stability test. M.L. recorded UV-Visible spectra at elevated temperatures. K.S. carried out TEM and XPS characterization. All made contributions to the manuscript preparation. Y.H.H. wrote the manuscript.

References

1. García-Lario, G. S. Grasa, R. Murillo, *Chem. Eng. J.,* 2015, **264**, 697-705.
2. J. H. Jeong, J. W. Lee, D. J. Seo, Y. Seo, W. L. Yoon, D. K. Lee, D. H. Kim, *Appl. Catal. A: General,* 2006, **302**, 151-156.
3. Y. H. Hu, E. Ruckenstein, *Catal. Rev.,* 2002, **44**, 423.
4. Y. H. Hu, E. Ruckenstein, *Adv. Catal.,* 2004, **48**, 298.
5. J. R. Rostrup-Nielsen, *Catal. Today,* 1993, **18**, 305-324.
6. A. Fujishima, K. Honda, *Nature,* 1972, **238**, 37-38.
7. X. Chen, L. Liu, P. Y. Yu, S. S. Mao, *Science,* 2011, **331**, 746-750.
8. X. Chen, S. Shen, L. Guo, S. S. Mao, *Chem. Rev.,* 2010, **110**, 6503-6570.
9. O. Khaselev, J. A. John, *Science,* 1998, **280**, 425-427.
10. Y. H. Hu, *Angew. Chem. Int. Ed.,* 2012, **51**, 12410-12412.
11. R. Asahi, T. Morikawa, T. Ohwaki, K. Aoki, Y. Taga, *Science,* 2001, **293**, 269-271.
12. X. Chen, C. Burda, *J. Am. Chem. Soc.,* 2008, **130**, 5018-5019.
13. J. H. Park, S. Kim, A. J. Bard, *Nano Lett.*, 2006, **6**, 24–28.
14. X. B. Chen, C. Li, M. Gratzel, R. Kostecki, S. S. Mao, *Chem Soc. Rev.,* 2012, **41**, 7909-7937.
15. M. R. Hoffmann, S. T. Martin, W. Choi, D. W. Bahnemann, *Chem. Rev.,* 1995, **95**, *69-96*.
16. M. Pelaez, N. T.Nolan, S. C. Pillai, M. K. Seery, P. Falaras, A. G. Kontos, P. S. M. Dunlop, J. W. J. Hamilton, J. A. Byrne, K'. O'Shea, M. H. Entezari, D. D. Dionysiou, *Appl. Catal. B,* 2012, **125**, 331-349.
17. S. Hoang, S. Guo, N. T. Hahn, A. J. Bard, C. B. Mullins, *Nano Lett.*, 2012, **12**, 26 -32.
18. B. Han, Y. H. Hu, *J. Phys. Chem. C*, 2015, **119**, 18927 -18934.
19. B. Han, W. Wei, L. Chang, Y. H. Hu, *ACS Catal.,* 2016, **6**, 494-497.
20. C. E. Taylor, *Catal. Today,* 2003, **84**, 9-15.
21. M. A. Gondal, A. Hameed, Z. H. Yamani, A. Arfaj, *Chem. Phys. Lett.,* 2004, **392**, 372-377.
22. (a) K. Shimura, H. Kawai, T. Yoshida, H. Yoshida, *ACS Catal.*, 2012, **2**, 2126-2134; (b) K. Shimura, H. Yoshida, *Energy Environ. Sci.,* 2010, **3**, 615-617.
23. (a) K. Shimura, K. Maeda, H. Yoshida, *J. Phys. Chem. C,* 2011, **115**, 9041-9047; (b) K. Shimura, S. Kato, T. Yoshida, H. Itoh, T. Hattori, H. Yoshida, *J. Phys. Chem. C,* 2010, **114**, 3493-3503.
24. G. A. Somorjai, K. R. McCrea, *Adv. Catal.,* 2000, **45**, 385-438.
25. G. Morin, D. Bonnin, *J. Magn. Reson.,* 1999, ***136***, 176-199.

Table of Contents Entry